Drug Delivery and Translational Research
https://doi.org/10.1007/s13346-020-00855-9

ORIGINAL ARTICLE

Enzymatically crosslinked tyramine-gellan gum hydrogels as drug delivery system for rheumatoid arthritis treatment

Isabel Matos Oliveira [1,2] · Cristiana Gonçalves [1,2] · Myeong Eun Shin [3] · Sumi Lee [3] · Rui L. Reis [1,2] · Gilson Khang [3] · Joaquim Miguel Oliveira [1,2]

Accepted: 7 September 2020

Abstract

Rheumatoid arthritis (RA) is a chronic inflammatory disease characterized by joint synovial inflammation, as well as cartilage and bone tissue destruction. Current strategies for the treatment of RA can reduce joint inflammation, but the treatment options still represent stability concerns since they are not sufficient and present a fast clearing. Thus, several drug delivery systems (DDS) have been advanced to tackle this limitation. Injectable gellan gum (GG) hydrogels, reduced by physical crosslinking methods, also being proposed as DDS, but this kind of crosslinking can produce hydrogels that become weaker in physiological conditions. Nevertheless, enzymatic crosslinking emerged as an alternative to increase mechanical strength, which can be adjusted by the degree of enzymatic crosslinking. In this study, tyramine-modified gellan gum (Ty-GG) hydrogels were developed via horseradish peroxidase (HRP) crosslinking; and betamethasone was encapsulated within, to increase the specificity and safety in the treatment of patients with RA. Physicochemical results showed that it was possible to modify GG with tyramine, with a degree of substitution of approximately 30%. They showed high mechanical strength and resistance, presenting a controlled betamethasone release profile over time. Ty-GG hydrogels also exhibited no cytotoxic effects and do not negatively affected the metabolic activity and proliferation of chondrogenic primary cells. Furthermore, the main goal was achieved since betamethasone-loaded Ty-GG hydrogels demonstrated to have a more effective therapeutic effect when compared with the administration of betamethasone alone. Therefore, the developed Ty-GG hydrogels represent a promising DDS and a reliable alternative to traditional treatments in patients with RA.

Keywords Rheumatoid arthritis · Hyperplasic synovium · Ty-GG hydrogels · Horseradish peroxidase · Drug delivery

Introduction

Rheumatoid arthritis (RA) is a chronic autoimmune disease, with a complex pathology that affects about 1% of the worldwide population [1, 2]. It is characterized by progressive chronic inflammation of joints and the proliferation of the synovium leading to pannus formation, bones, and cartilage destruction. It is associated with persistent arthritic pain, swelling, stiffness, and work disability. RA is also responsible for the decreased expectancy and quality of life, being more prevalent in women than men [3, 4].

Despite the recent advances in medical therapeutics, currently, it is only possible to slow down the progression of the disease and attempt to increase the quality of life, being not possible to cure RA. The most commonly used therapeutic agents for RA include disease-modifying anti-rheumatic drugs, glucocorticoids, non-steroidal anti-inflammatory drugs, and biological agents. However, such therapies have several drawbacks due to quite a few side effects, such as headaches, dizziness, insomnia, damage to the skin and hair, cytopenia, and transaminase elevation, among others, mainly caused by the lack of selectivity of the drugs and also frequent and long-term dosing that lead to patient non-compliance [5, 6].

✉ Joaquim Miguel Oliveira
miguel.oliveira@i3bs.uminho.pt

[1] 3B's Research Group, I3Bs - Research Institute on Biomaterials, Biodegradables and Biomimetics of University of Minho, Headquarters of the European Institute of Excellence on Tissue Engineering and Regenerative Medicine, Avepark, Parque de Ciência e Tecnologia, Zona Industrial da Gandra, 4805-017 Barco, Guimarães, Portugal

[2] ICVS/3B's - PT Government Associate Laboratory, /Guimarães, Braga, Portugal

[3] Department of BIN Fusion Technology, Department of Polymer Nanoscience and Polymer BIN Research Centre, Chonbuk National University, 567 Baekje-daero, Deokjin-gu, Jeonju 561-756, Republic of Korea

Published online: 13 September 2020

A possible solution to avoid the undesired side effects is the drug delivery directly to the affected site, via intra-articular injection.

Compared with traditional methods currently used for the administration of drugs, the use of biomaterials as drug delivery systems present many advantages. Those advantages are related, for instance, with the improvement of the insoluble drug delivery, maximizing the bioavailability, and the treatment efficacy. Furthermore, the use of biomaterials can help to reduce secondary effects and enhance the plasma half-life of peptide drugs by protecting them from degradation caused by the environment [7, 8].

Hydrogels are three-dimensional, crosslinked networks of water-soluble polymers that have physiochemical similarities to the extracellular matrix, namely, mechanical and composition properties. The particular physical properties of hydrogels have encouraged the interest in their use in drug delivery applications. The porosity of the hydrogels also enables the charging of drugs into the gel matrix and posterior controlled drug release [9, 10].

An injectable hydrogel is a class of hydrogel, which can convert from solution to gel in situ upon physical or chemical stimuli. Therefore, these hydrogels can be introduced into a defined position of the body through a minimally invasive method [11, 12].

Gellan gum (GG) is a bacterial polysaccharide obtained from *Sphingomonas elodea*, and its glycosidic backbone is a repeating tetrasaccharide unit with one L-glycerate per repeating unit and one acetate, occurring every two sequences as esterified substituents [13]. GG is biodegradable, biocompatible, and non-toxic. In tissue engineering, the versatility of this polysaccharide has been studied to develop drug delivery systems such as the development of injectable hydrogels [14]. Physical crosslinking methods can produce GG hydrogels that become weaker in physiological conditions since a switch of divalent cations by monovalent ones and physically crosslinked hydrogels occur, leading to the loss of in vivo stability after implantation [15, 16]. Enzymatically crosslinked hydrogels, including covalent bonds between the polymer chains, are produced via radical polymerization and non-enzymatic or enzymatic crosslinking of complementary groups [17, 18]. Enzyme-mediated hydrogel formation is a suitable method of crosslinking materials in the aqueous medium due to the reaction condition desirable near physiological pH and room temperature. Furthermore, enzymatic hydrogelation prevent the production of undesirable by-products or cytotoxic composite because enzymes only work with distinct substrates [19, 20].

Enzymatic crosslinking of polymer-phenol conjugates in the presence of horseradish peroxidase (HRP) and H_2O_2 has emerged as a valuable method to synthesize in situ forming (injectable hydrogels) due to fast gelation and controllable crosslinking density [21, 22]. Furthermore, HRP has moderate substrate specificity and can easily be a tuned hydrogel network by adjusting the concentration of enzyme and subtract [19, 23]. Several research groups reported the in situ formation of hydrogels through the functionalization of polymers with tyramine. The hydrogels are chemically crosslinked and consequently possess superior characteristics in terms of stability and mechanical resistance when compared with physically crosslinked and been widely used in drug delivery [24].

In this work, it was developed tyramine-modified gellan gum (Ty-GG) hydrogels (crosslinked by both physical and chemical mechanisms) in the presence of horseradish peroxidase (HRP) and hydrogen peroxide (H_2O_2). The Ty-GG hydrogels were loaded with betamethasone in order to provide its sustain release and improve the treatment safety in patients with RA. Physicochemical characterization was performed to evaluate the successful functionalization of Ty-GG using nuclear magnetic resonance (^{1}H-NMR) and Fourier-transform infrared (FTIR) spectroscopic techniques. Furthermore, the betamethasone-loaded Ty-GG hydrogel water uptake, weight loss, gelation time, injectability, and rheological properties were assessed. The betamethasone release profile from the Ty-GG hydrogels was also evaluated in vitro. In vitro studies for cell viability such as 3-(4,5-dimethylthiazol-2-yl)-2,5-diphenyl-2H-tetrazolium bromide and DNA proliferation on chondrogenic primary cells and anti-inflammatory activity by enzyme-linked immunosorbent in THP-1 cell line were performed.

Materials and methods

Synthesis of tyramine-gellan gum

The functionalization of gellan gum with tyramine was carried out following the method reported by Prodanovic et al. [25], with minor changes. Briefly, gellan gum from Gelzan™ CM (Sigma-Aldrich, USA) was dissolved in water at 90 °C to a final concentration of 1% (w/v). Sodium (meta)periodate (Sigma-Aldrich, USA) was added to a final concentration of 1 mM in GG at 1% (w/v). The reaction was kept in the dark for 24 h at 4 °C. The reaction was then stopped by adding glycerol (500 mM) and incubated for 30 min in the dark at 4 °C. The oxidized GG was precipitated from the reaction mixture by adding NaCl at 1% (w/v) and 2 volumes of 99% (v/v) ethanol. This precipitation step was repeated two times, using the same procedure after dissolving oxidized GG at 1% (w/v) concentration in water. In the end, the precipitate was separated, dried, and dissolved in 0.1 M sodium-phosphate buffer pH 6. When dissolved at 1% (w/v) concentration, tyramine hydrochloride (Sigma-Aldrich, USA)

was added by molecular equivalents (number of mol equivalents of GG to number of mol equivalents of tyramine), and the solution was stirred for 30 min. Subsequently, solid cyanoborohydride was added at 0.5% (w/v) final concentration, and the reaction mixture was left in the dark for 24 h at 4 °C. Modified gellan gum was precipitated by adding NaCl to 1 M final concentration and two volumes of 96% (v/v) ethanol. Precipitation was repeated two times using the same procedure after dissolving modified GG at 1% (w/v) concentration in water. Ty-GG powder was obtained by lyophilization, at 0.08 mbar and − 77.7 °C, during approximately 4 days.

Physicochemical characterization

Fourier-transform infrared spectroscopy

Powder samples of Ty-GG, GG, and tyramine were mixed with potassium bromide, and, using a manual press, a transparent pellet was obtained. The transmission spectra of the samples were obtained on an IR Prestige-21 spectrometer (Shimadzu, Japan), using 32 scans, a resolution of 4 cm^{-1}, and a wavenumber range between 4400 and 400 cm^{-1}.

Assessment of the degree of substitution of tyramine in gellan gum

The chemical modification of GG with Ty was evaluated and quantified by proton nuclear magnetic resonance spectroscopy (^{1}H-NMR). Ty-GG was solubilized in deuterium water oxide (D_2O) (2 mg mL^{-1}) at room temperature. Then, 1 mL of the sample was transferred to an NMR tube. The NMR spectra were obtained on a Bruker AVANCE 400 spectrometer, at 50 °C using a resonance frequency of 400 MHz. To process and analyze the obtained spectra, MestReNova 9.0 Software was used. The degree of substitution (DS, the fraction of modified hydroxyl groups per repeating unit) was determined by the relative integration of the tyramine peaks ($I_{T1,T2}$ in Fig. 1) of the modified groups to methyl protons of the internal standard (I_{CH3} in Fig. 1), according to Eq. 1, adapted from another DS calculation as reported in several studies [26, 27]. The $n_{HT1,\ T2}$, and n_{HCH3} correspond to the number of tyramine protons and the methyl protons of GG monomer, respectively. $^{n}{}_{OH}$ corresponds to the number of reactive -OH sites in the GG structure.

$$DS = \left(\frac{\frac{I_{T_1 T_2}}{I_{CH_3}}}{\frac{n_{H T_1 T_2}}{n_{CH_3}}} / n_{OH} \right) \times 100 \quad (1)$$

Horseradish peroxidase to induce tyramine-gellan gum hydrogels formation

Horseradish peroxidase (HRP) solution (0.84 mg mL^{-1}) (Sigma-Aldrich, USA) and hydrogen peroxide solution (H_2O_2) (0.36% (v/v)) (VWR, USA) were both prepared in water. Tyramine-gellan gum solution of 1% (w/v) was used for the hydrogel preparation. Tyramine-gellan gum hydrogels were prepared by mixing of Ty-GG solution with different amounts of HRP and H_2O_2 solutions (Table 1**)**. Ty-GG hydrogel discs were prepared by adding 200 μL of the mixture solutions in a polypropylene mold at 37 °C.

Water uptake and weight loss of the tyramine-gellan gum hydrogels

Weight loss and water uptake of Ty-GG hydrogels were performed. Hydrogels were soaked into a PBS solution at 37 °C, for up to 21 days, in triplicate. Then, specimens were removed after the different time points of immersion. The initial weight (W_i) of each sample was measured, and then Ty-GG hydrogels were immersed in PBS solution. At each time point, the samples were removed and put in a filter paper to remove the excess of the solution, and the wet weight (W_W) was measured. The water uptake was determined as shown in Eq. 2.

$$\text{Water uptake } (\%) = \frac{w_w - w_i}{w_i} \times 100 \quad (2)$$

The weight loss was quantified after the samples were dried at 70 °C and until they reached constant weight (W_f), using Eq. 3.

$$\text{Weight loss } (\%) = \frac{w_i - w_f}{w_i} \times 100 \quad (3)$$

Investigation of gelation time, injectability tests, and rheological properties

The vial inversion test was routinely used to determine an approximate gelation time. Thereby, after mixing Ty-GG with HRP and H_2O_2, the vials were placed in the water bath at 37 °C and then inverted to see how long it takes to turn to gel.

The injectability tests were also investigated by means of injectability measurement equipment (PARALAB). The injectability measurements were performed using a syringe with a 27 G needle. The material was placed in the syringe that was placed in the equipment, and then it applied a force that extruded the sample from the syringe at a rate of 1 ml min^{-1}. The force needed for each hydrogel condition was

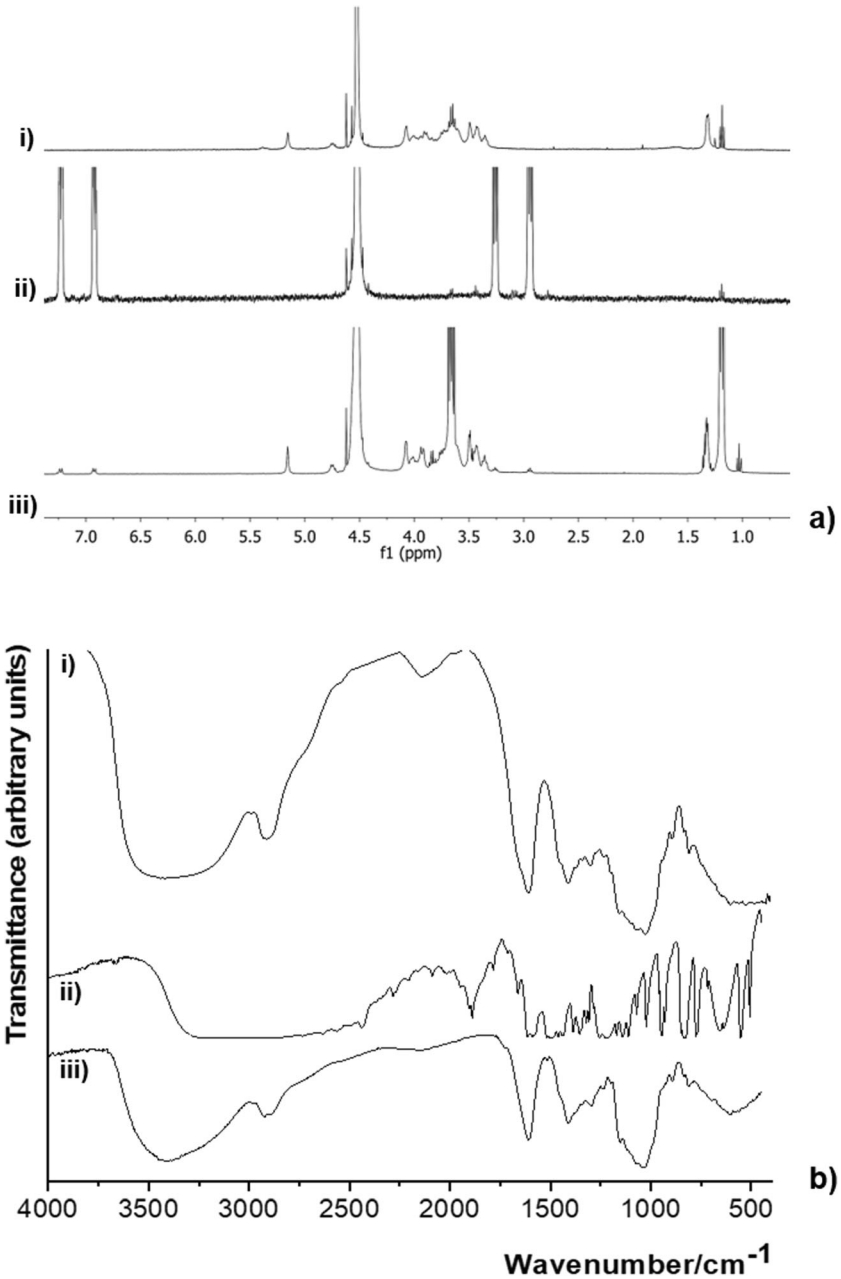

Fig. 1 ^{1}H-NMR spectra (**a**) of GG (i), tyramine (ii), and the obtained Ty-GG (iii) in D_2O at 50 °C. FTIR spectra (**b**) of GG (i), tyramine (ii), and Ty-GG (iii)

recorded. Triplicates of each sample were performed, and water was used as a control.

The mechanical properties of Ty-GG hydrogels were evaluated by using a rheometer (Kinexus pro+rheometer, software rSpace, from Malvern). The oscillatory experiments were performed using a stainless-steel plate-plate measuring system. This system is composed of an upper stainless-steel plate of 8 mm diameter, with a rough finish to prevent the sample from slipping. Frequency sweep curves, also known as mechanical spectra, were obtained from 0.01 to 1 Hz of frequency, at a shear strain of 0.1% (from LVER determination) for 5 min at 37 °C. These curves were obtained in three independent tests, with different samples of the same condition.

Table 1 Ty-GG conditions (C1, C2, and C3) with different amounts of HRP and H_2O_2 solutions

	Ty-GG	HRP	H_2O_2
C1	167 μL	16.6 μL	10.83 μL
C2	167 μL	18.3 μL	15 μL
C3	167 μL	20 uL	13.3 μL

Drug release profile of the betamethasone-loaded tyramine-gellan gum hydrogels

To assess the drug release system, one corticosteroid, betamethasone, was incorporated in Ty-GG hydrogels. Ty-

GG hydrogels loaded with betamethasone (Sigma-Aldrich, USA) were prepared by mixing Ty-GG solution, with 5 mg mL^{-1} of betamethasone in PBS, and the enzymatic crosslinking was made by adding of HRP and H_2O_2. Betamethasone release profile in Ty-GG 1% hydrogels was evaluated immersing each hydrogel in PBS at 37 °C. After each time point (3 h, 6 h, 24 h, 72 h, 168 h, 336 h and 504 h), the supernatant was removed and kept at − 80 °C until the end of the experiment. Three samples per condition were used at each time point. To formulate the calibration curve, betamethasone dilutions were prepared (from 0 to 5 mg mL^{-1}). The UV absorbance at 490 nm was read in a microplate reader (EMax; Molecular Devices, Sunnyvale, CA, USA) to measure the betamethasone release.

In vitro studies

Cell culture

Chondrogenic primary cells isolated from female New Zealand White rabbits (Damul Sci., Korea) with 1 kg and 6 weeks were used. Dulbecco's modified eagle medium (DMEM/ F12) (Gibco, USA) was used in chondrogenic cells. This culture medium was supplemented with 10% (v/v) fetal bovine serum (Gibco, USA) and 1% (v/v) antibiotic-antimycotic (Gibko/Thermo Fisher Scientific, South Korea) under standard conditions (37 °C in a humidified atmosphere containing 5% CO_2). Human monocytic cell line (THP-1) (SIGMA, USA) was expanded in RPMI 1640 Medium, GlutaMAX™ Supplement, HEPES (Thermo Fisher Scientific, USA), supplemented with 10% fetal bovine serum and 1% (v/v) of penicillin and streptomycin, under standard culture conditions (37 °C in a humidified atmosphere containing 5 vol% CO_2).

Chondrogenic cell isolation

Chondrogenic primary cells were isolated from rabbit cartilage. The knees were initially removed from the rabbit, and the samples were washed 3 times with PBS (1X) solution. The cartilage was scraped carefully with the blade, and small fragments were placed inside a conical tube with 1.5% (v/v) antibiotic-antimycotic. The sample was centrifuged at 300 G, 3 min and 4 °C. The supernatant was discarded and refilled with an enzymatic cocktail (DMEM/F12 medium + collagenase A (Roche, USA). The solution was previously filter-sterilized through a 0.2 μm filter. The sample was placed in the CO_2 incubator at 37 °C for 24 h. The next day, cells were centrifuged at 300 G, for 3 min and at 4 °C. The supernatant was removed, and the cells were plated on a cell culture dish, with a complete medium and kept in the CO_2 incubator at 37 °C until they reach the desired confluence.

Metabolic activity

The metabolic activity of chondrogenic primary cells was assessed by MTT assay following the MEM extract test. The MEM extract test protocol followed was established according to the European and international standards.

The Ty-GG hydrogels (C1, C2, and C3 (previously described)) were prepared with a thickness ranging from 0.5 to 1 mm, a minimum area of 60 cm^2. The samples were placed in a sterile tube with 10/20 mL of cell culture medium, and they were kept in the water bath at 37 °C and 60 rpm for 24 h. Parallel 200 μL cell suspension was transferred into 96-well plates to obtain a cell density of 10,000 cells per cm^2. After 24 h of incubation, the extraction fluid was passed through a 0.45 μm membrane filter, and the medium of cells was removed and replaced with the extraction fluid. Cells with DMEM-F12 medium were used as control.

The cell cultures were evaluated by 3-(4,5-dimethylthiazol-2-yl)-2,5-diphenyltetrazolium bromide (MTT, Sigma, South Korea) at 24, 48, and 72 h. At each time point, the DMEM/F12 medium was replaced by culture medium containing MTT assay in a 9:1 ratio and incubated for 3 h. When violet crystals were formed, they were melted using dimethyl sulfoxide solution (DMSO). Then, 100 μL of solution from each well was transferred to 96-well plates, and a microplate reader (EMax; Molecular Devices, Sunnyvale, CA, USA) was used at 570-nm optical density.

DNA quantification

The total amount of DNA was assessed using DNA quantification kit (Quant-iT™ PicoGreen® dsDNA Assay Kit, Invitrogen, USA), to evaluate the effect of Ty-GG hydrogels in chondrogenic primary cells. The cells were seeded at a density of 10,000 cells per cm^2 and incubated with extraction solution of Ty-GG hydrogels (C1, C2, and C3) for periods of 24, 48, and 72 h. After the incubation period of the cells, they were washed with PBS solution and were lysed with water pure water. The cell solution was placed into microtubes, incubated for 1 h in a water bath at 37 °C, and then they are stored at − 80 °C for further analysis. Cells cultured with DMEM-F12 medium were used as a positive control. Several solutions were prepared, with concentrations ranging from 2 to 0 μL mL^{-1} to plot a DNA calibration curve. In each well (of the 96-well opaque plate), 28.7 μL of each sample or standard was mixed with 71.3 μL of PicoGreen solution and 100 μL 1X TE. Then, the plate was incubated in the dark for 10 min, the fluorescence was read using excitation of 480/20 nm and emission of 528/20 nm in a microplate reader, and DNA concentration was determined from the standard curve.

Fluorescence microscopy

Chondrogenic primary cells were seeded using the same protocol and conditions described above. Then, cells were fixed with 10% formalin (Sigma-Aldrich, USA) and stained with Texas Red-X phalloidin (Sigma-Aldrich, USA) for actin filaments of the cytoskeleton and 4,6-diamidino-2-phenylindole, dilactate (DAPI blue, VWR International, USA) for nuclei. At the end, cells were analyzed under the fluorescence microscope (Axiolmager, Z1, Zeis Inc., Oberkochen, Germany).

Anti-inflammatory activity of betamethasone-loaded Ty-GG hydrogels

The anti-inflammatory activity of betamethasone-loaded Ty-GG hydrogels was investigated with a THP-1 cell line. For this assay, the two concentrations that obtained the best results in metabolic activity and cell proliferation were evaluated. First, THP-1 cell line was seeded (1×10^6 cells per mL) and differentiated into macrophage phenotype with 100 nM phorbol 12-myristate 13-acetate (PMA) (Sigma-Aldrich, USA) for 1 day. The next day, the non-adhered cells were removed, the medium replaced, and new RPMI medium without PMA was added, for 2 days. THP-1 cells were incubated for 5 h with 100 ng mL^{-1} of lipopolysaccharide (LPS) (Sigma-Aldrich, USA) in RPMI medium to enable the inflammatory response. After incubation time, cells were cultured with two concentrations of betamethasone-loaded Ty-GG hydrogels (C1 and C2) for 7 days. Cells without treatment and differentiated with PMA and without LPS stimulation were used as control. At each time point (1 day, 3 days, and 7 days), the solution was collected and kept at − 80 °C for further analysis. Human TNF-alpha DuoSET ELISA (R&D Systems, USA) kit and DuoSet Ancillary Reagent Kit 2 (R&D Systems, USA), for the optimum performance of the ELISA kit, were used to assess the anti-inflammatory activity. The assay was performed to evaluate the system effectiveness through cytokine TNF-α. The TNF-α standards were prepared with concentrations ranging from 1000 to 0 pg mL^{-1} to make a TNF-α calibration curve. A microplate reader set (Synergy HT, BIO-TEK) at 450 nm was used to determine the optical density of each well.

Statistical analysis

GraphPad Prism 8 version was used to conduct the statistical analysis, where a Shapiro-Wilk normality test was formerly performed to evaluate the data normality. Non-parametric Kruskal-Wallis test was applied in all assays, except for weight loss and MTT assay where one-way ANOVA was used, since there was an absence of normality. Dunn's multiple comparison test was used to compare the mean rank of each condition with the mean rank of every other condition in non-parametric Kruskal-Wallis. Tukey's multiple comparison test was used to compare the mean of each condition with the mean of every other condition in one-way ANOVA. Statistical significances were determined as $*p < 0.05$, $**p < 0.01$, and $***p < 0.001$. All tests were performed in triplicated, and results were presented with mean ± standard deviation.

Results and discussion

Physicochemical properties

Ty-GG hydrogels were obtained via enzymatic crosslinking with HRP and H_2O_2 and encapsulated with betamethasone to increase the specificity and safety in the treatment of chronic inflammation of synovial joints in the patients suffering of RA. Ty-GG was synthesized by amide bond formation between the amine group of tyramine and the carboxyl group of GG. After the modification of GG with Ty, its efficacy was evaluated by NMR and FTIR analysis. Figure 1 shows a representative NMR spectrum (a) and FTIR spectra (b) of gellan gum, tyramine, and Ty-GG.

From Fig. 1a, it is possible to see that Ty-modified gellan gum (Ty-GG) (iii) showed additional peaks not appearing in the unsubstituted GG (i). The tyramine spectrum (ii) showed the distinctive signals for both pairs of aromatic ring protons (β pair and λ pair between 7.4 and 7.1 ppm) and aliphatic side chain protons between 3.4 and 3.1 ppm (α pair). These peaks are seen in Ty-GG spectrum and confirm the presence of tyramine on Ty-GG [28, 29].

The degree of substitution of GG with tyramine was calculated using Eq. 1. The obtained degree of substitution for Ty-GG is (30.2 ± 1.3) %. This value of the degree of substitution is higher when compared with other molecules modified with tyramine [30, 31].

From Fig. 1b, the GG and Ty-GG spectra within the region 1800–1200 cm^{-1} also indicated the efficient modification of tyramine-gellan gum. From the spectra analysis, it was possible to confirm the presence of the aromatic rings, due to the appearance of a peak of C-C (in-ring) stretching vibrations at 1517 cm^{-1} and 1417 cm^{-1}, only in the spectra of modified gellan gum, which is in accordance with the spectra found in the literature [25, 32].

It is known that ionic crosslinked hydrogels present weak mechanical proprieties [33]. This limitation can be overcome by modification of GG with tyramine, by enzymatic crosslinking. Therefore, enzymatic but also physical and chemical crosslinkings were combined to produce Ty-GG hydrogels with tunable mechanical proprieties.

Ty-GG hydrogels were produced via enzymatic crosslinking, with the enzyme HRP. Different conditions of Ty-GG hydrogels were produced and assessed (C1, C2, and

C3) regarding water absorption capacity and weight loss. Figure 2 shows the water uptake and weight loss of C1, C2, and C3 of Ty-GG hydrogels after soaking up to 504 h.

It was possible to verify that all conditions of Ty-GG hydrogels showed negative values of water uptake. The swelling ratios of gels ranged from (− 42.89 ± 6.25) %, (− 47.25 ± 1.47) %, (− 39.21 ± 1.53) % in the C1, C2, and C3, respectively. Some studies [11, 26] demonstrated that the crosslinking degree, the formation of ionic bonds, and hydrophilicity of network of hydrogels influence the swelling. In the swelling kinetics assays, the hydrogel behavior is powerfully influenced by the presence of cations in the immersion solution [11]. These cations form ionic bonds that increase the crosslinking degree and lower the water uptake ratio. Interactions between the carboxylic group on GG and calcium ions can reduce the hydrogen binding donors and receptors free for interaction with water, thereby decreasing the quantity of water related with the hydrogel network [34].

The results are in agreement with the previously mentioned studies [26, 34, 35]; the Ty-GG hydrogels produced by enzymatic crosslinking, after immersion in PBS (ionic crosslinking), did not present water absorption capability. Thus, it is possible to consider this test as an indirect method to assume a high crosslinking degree in the produced gels,

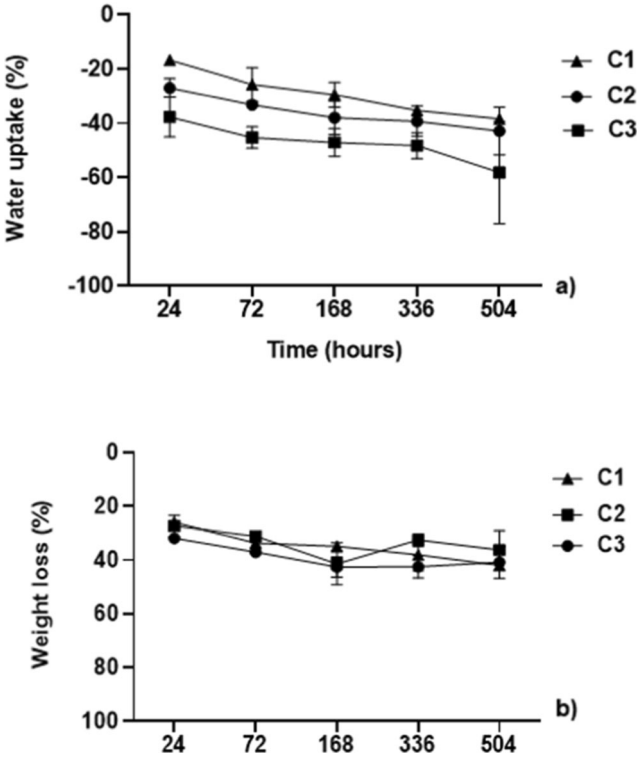

Fig. 2 Water uptake (**a**) and weight loss (**b**) of Ty-GG hydrogels after 24 h, 72 h, 168 h, 336 h, and 504 h of soaking. Significant differences ***$p < 0.001$, **$p < 0.01$, and *$p < 0.05$. Water uptake, significant differences between (C2 vs C3) *$p < 0.05$ at time point 1 day and 3 days, non-parametric Kruskal-Wallis test. Weight loss, significant differences between (C1 vs C2) **$p < 0.01$ at time point 3 days, one-way ANOVA

thus showing that the properties of GG improved after modification.

The degradation profile of hydrogels in this study was obtained by exposing the Ty-GG hydrogels in PBS at different points (Fig. 2b). The weight loss results show that all concentrations had approximately the same degradation profile over time. The weight loss ratio was (40.8 ± 4.1) %, (36.2 ± 0.7) %, and (41.9 ± 1.6) %, for C1, C2, and C3, respectively. Ty-GG hydrogels are relatively stable in PBS due to the ionic crosslinking, being possible to observe a similar weight loss rate over time. The osmotic forces influence this process, such as the external ionic aqueous solution and the elastic force executed by the crosslinked polymeric structure [36]. When the external solution is ionically more concentrated than the hydrogels, the ions can penetrate the hydrogels. Consequently, the hydrogel crosslinking degree is stabilized and increased, being the water molecule expulsion stimulated and consequently the weight loss decreased. Furthermore, the ionic crosslink, when combined with chemical crosslink mechanisms extend the rate of degradation, as reported by several studies [26, 35].

The gelation time is a crucial parameter for the formation of hydrogels in situ and is widely connected with the crosslinking rate of the HRP-catalyzed reaction [23]. The gelation time was determined by the vial inversion test. After adding Ty-GG with HRP and H_2O_2, the vials were placed at 37 °C in the water bath and then inverted. It was possible to verify that all concentrations (C1, C2, and C3) had a gelation time about 30 s.

Several studies reported that HRP catalyzes the crosslinking reaction of polymer-phenol conjugates in the presence of H_2O_2, resulting in hydrogels with tunable gelation rate [20]. The HRP and H_2O_2 concentrations are essential parameters to control the crosslinking rate of phenol-rich polymers. The association between these parameters and gelation time has been well-known. It has been described that the gelation time reduced with rising HRP concentration [37, 38]. In order to use injectable hydrogels for bio-applications, a suitable gelation time is desired. A short gelation time (10 s to a few minutes) is essential for efficient local delivery of drugs [31, 39]. While a quick gelling time is beneficial to obtain high loading efficiency of drugs in hydrogels, in a real clinical setting, rapid administration can be more challenging. The use of appropriate syringes, with more than one channel, in which the mixture is made while the injection is given, would be the most appropriate form of administration. Through the results obtained, it was possible to confirm that the produced gels fulfill the necessary characteristics.

The injectability (formulation performance during injection, including pre-filled syringes) is a very important parameter to determine the force required to extrude the material through a device [40]. The injectability analysis was performed for the three conditions of hydrogels (C1, C2, and C3), and water was used as control. The syringe was loaded

with the Ty-GG solution, HRP, and H_2O_2 to form the hydrogels, and the injection was performed using a rate of 1 mL min^{-1}. The force needed for each injection was measured, together with the control (water), and is presented in Fig. 3.

In Fig. 3, it was visible that the force needed to inject the condition 1 (5.2 ± 0.3) N and condition 2 (4.9 ± 0.2) N is greater than the force required to inject water (3.9 ± 0.1) N. However, the force required to inject condition 3 (4 ± 0.1) N is comparable with the force required to inject water. Initially, in condition 1, there was a lower value in the injectability force, with that force increasing around 23 s, possibly due to the beginning of the crosslinking in the reaction, and then the value remained constant until the end of the analysis. In condition 2, the same profile of injectability as in condition 1 was observed, although the values of the injectable force were lower, and the increase of force occurred around 31 s. This result may be due to condition 1 having a slightly higher degree of crosslinking when compared with condition 2; therefore, there is a slight difference in behavior. In condition 3, there was an injectability force value similar to the value obtained with water. However, in condition 3, there was also an increase in the injectable force around 31 s, which, like the other conditions, maybe due to the beginning of the crosslinking of the reaction. Taking this into account, condition 3 has presented an injectable force more similar to that found in water, meaning that it can become easier and less painful to inject into the patient. However, conditions 2 and 3, despite having higher injectable force values, may have other advantages as was verified in other characterization tests.

The mechanical properties of Ty-GG hydrogels were assessed after enzymatic crosslinking via HRP and stabilized at different time points in PBS. The hydrogels were evaluated through oscillatory rheology experiment at 37 °C. The oscillatory shear flow has been extensively used to measure viscoelastic properties of materials. The storage modulus, elastic solid-like behavior, (G`), provides a small amplitude of oscillatory shear and loss modulus, and the viscous response, (G``),

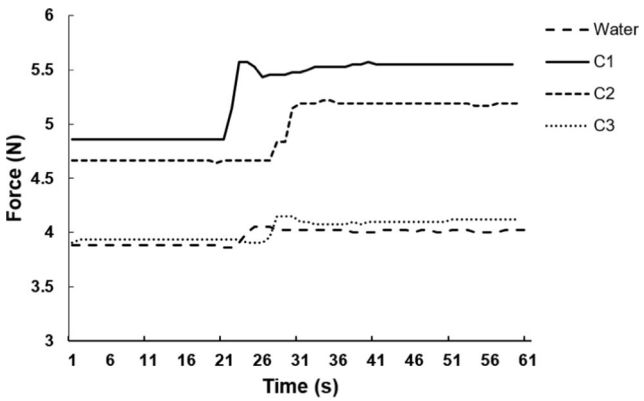

Fig. 3 Injectability test of Ty-GG hydrogels, C1, C2, and C3, and water (control). Significant differences ***$p < 0.001$ (water vs C1) and (water vs C2), non-parametric Kruskal-Wallis test

assesses stress amplitude and the time lag between the stress and strain. The phase angle (δ, $0 \leq \delta \leq 90°$) is a representative physical property that estimates the viscoelasticity of a material. G`, G``, and δ are determined by a single function of the frequency (f). These materials are often called linear viscoelastic properties. A general form of the shear stress subjected to oscillatory shear ($\lambda = \lambda_0 \sin\omega t$) [41]. Figure 4 shows the mechanical spectra of Ty-GG hydrogels (C1, C2, and C3), after different time points.

The spectrum of mechanical proprieties of Ty-GG hydrogels showed that at 24 h and 72 h, all conditions of Ty-GG hydrogels demonstrated a G`` > G` and consequently presented a high phase angle, that is, a viscous component higher than the solid. In the following time points, 168 h, 336 h, and 504 h, it was possible to observe that the phase angle decreased, G` > G``, so the elastic component is higher than the viscous component, showing that the material has a viscoelastic behavior, with superior elastic character [41, 42]. The Ty-GG hydrogels are intended to be injected in the synovial cavity filled with synovial fluid. This fluid has highly viscous (G`` > G`) properties, and the hydrogels obtained showed viscoelastic behavior with high viscosity after formation, similar to the synovial liquid. Thus, Ty-GG hydrogels achieved the desired mechanical properties [43, 44]. Viscoelastic materials, such as the proposed Ty-GG hydrogels, can be injected directly into the knee joint of patients with RA and, in addition to function as a drug carrier, surrounding the deficient cartilage joints and acting as a lubricant and shock absorber [45], as well as reducing pain and slowing down the disease progress.

Controlled drug delivery is revealing great importance over conventional drug delivery methods. In traditional drug administration, drug concentration in the blood rises instantly after the drug is taken and then decreases over time. Plasma drug concentration is a vital parameter for any drug since there is an optimum concentration above which it is toxic and below which it is not effective. The conventional drugs are also very limited concerning their short half-lives and their stability only under physiological conditions. Therefore, drug delivery at a constant rate is generally better compared with the traditional methods of drug administration [46–48].

Betamethasone suspensions were approved for intra-articular injection to provide adjuvant therapy in rheumatoid arthritis. Normal intra-articular doses of betamethasone suspensions differ with the size of the joint, from 1.5 to 12 mg [49]. In this work, 5 mg mL^{-1} of betamethasone was used because it was the average value found in the literature to have a therapeutic effect. The betamethasone has a short half-life about 36–54 h [50], which means that the drug must be injected more frequently to have the desired therapeutic effect. It was possible to verify that the Ty-GG hydrogels allowed a controlled release profile of betamethasone over 21 days, not reaching the maximum of release in any of the concentrations,

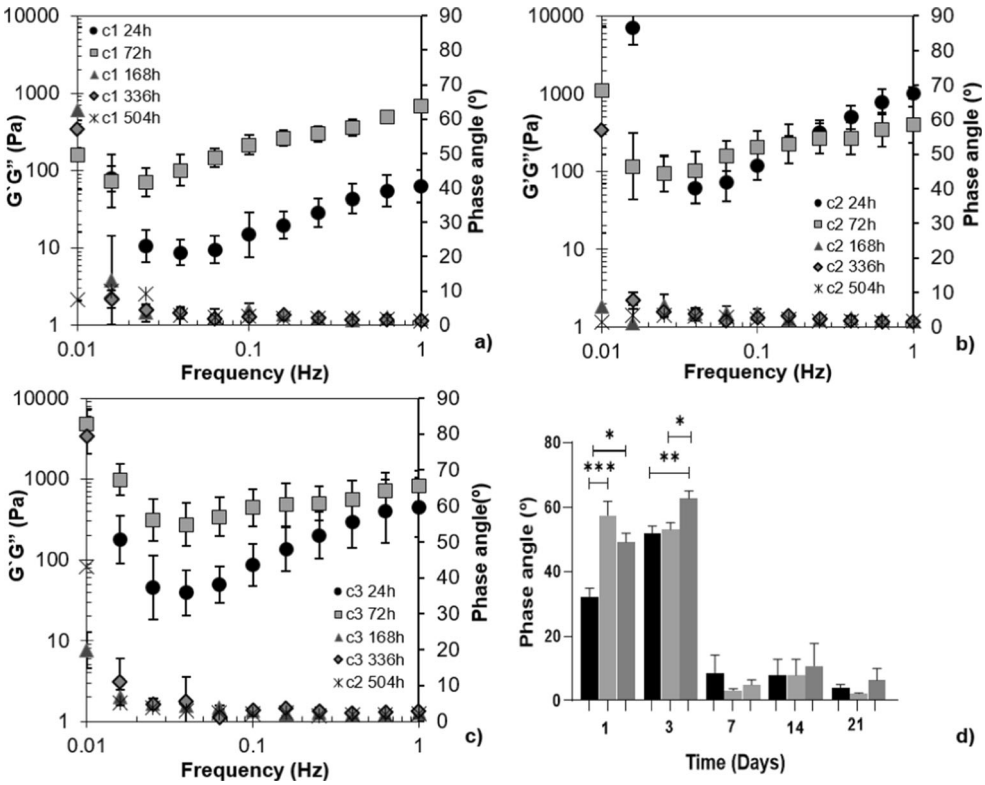

Fig. 4 Mechanical spectra of Ty-GG hydrogels: C1 (**a**), C2 (**b**), and C3 (**c**) at different time points (24 h, 72 h, 168 h, 336 h, and 504 h). Significant differences ***$p < 0.001$, **$p < 0.01$, and *$p < 0.05$, non-parametric Kruskal-Wallis test

C1 released (64 ± 1.5) % of the drug, C2 released (51 ± 0.8)%, and C3 released approximately (82 ± 0.05)% (Fig. 5). Intra-articular corticosteroid therapy has been used for the treatment of RA. Corticosteroid therapy is effective at temporarily alleviating joint symptoms associated with inflammatory disorders. However, long-term adverse effects of corticosteroids on chondrocyte of the articular cartilage are a concern. Thus, the number of injections is usually restricted [51, 52]. The use of Ty-GG hydrogels loaded with betamethasone allows the drug to be administered less frequently, providing lower and continuous dosages of the drug, thus decreasing the levels of toxicity. In addition, constant injections can become painful and uncomfortable for patients. Thus, the use of Ty-GG hydrogels to betamethasone release can improve the failures of the traditional models, allowing a better quality of patient's life during the treatment period.

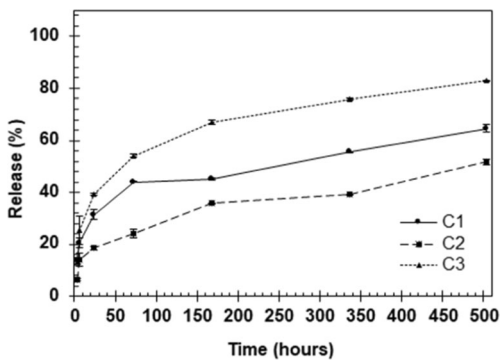

Fig. 5 Drug release profile of Ty-GG hydrogels (C1, C2, and C3) with encapsulated betamethasone for 3 h, 6 h, 24 h, 72 h, 168 h, 336 h, and 504 h. Significant differences ***$p < 0.001$, **$p < 0.01$, and *$p < 0.05$, by non-parametric Kruskal-Wallis test. At time point 1 day, significant differences between (C2 vs C3) *$p < 0.05$, at time point 3 days (C2 vs C3) *$p < 0.05$, at time point 14 days (C1 vs C2) *$p < 0.05$

In vitro studies

Cell viability and proliferation of Ty-GG hydrogels were assessed in chondrogenic primary cells, and therapeutic efficacy was evaluated using the THP-1 cell line.

MTT assay was made to investigate the influence of Ty-GG hydrogels. Thus, the metabolic activity of cells up to 72 h of culturing (Fig. 6a) was evaluated. DNA quantification was also performed to assess cell proliferation (Fig. 6b).

From day 1 to day 3, all cells with different conditions of Ty-GG hydrogels have shown an increase of metabolic activity, not presenting significant differences between them. However, on day 2, cells with C3 demonstrated significant differences as compared with control (*$p < 0.05$).

In parallel, DNA quantification was performed to assess cell proliferation for 72 h. It was observed that there was a decrease in the first time point in C2 and C3 samples, although there were no significant differences. At the following time points, there was an increase in cell proliferation in all conditions, and no significant differences were found between conditions.

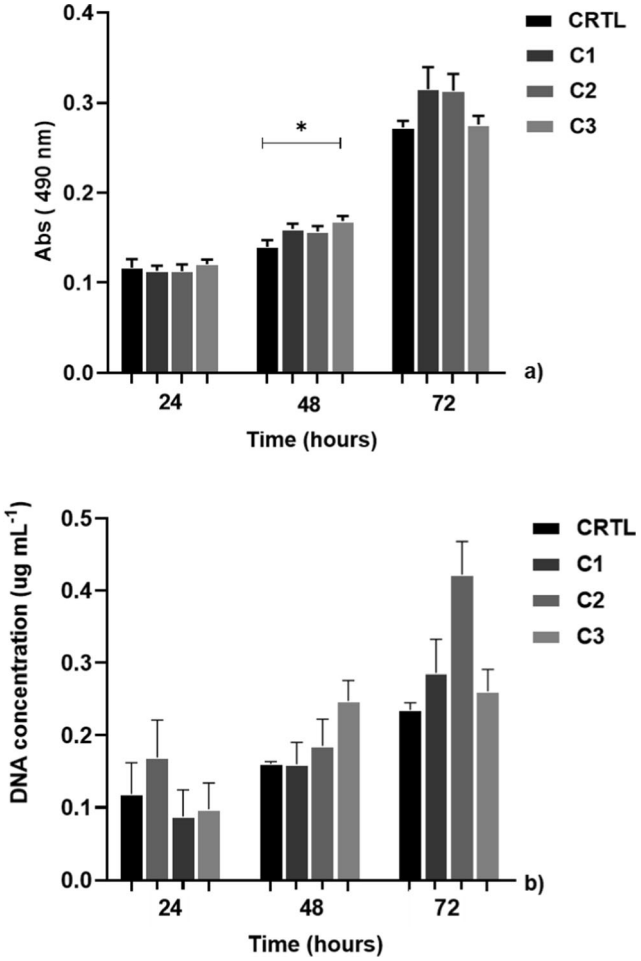

Fig. 6 MTT assay (**a**) and DNA quantification (**b**) of chondrogenic primary cells with control (cells with DMEM-12 medium) and different conditions (C1, C2, and C3) of Ty-GG hydrogels, after 24 h, 48 h, and 72 h of culturing. Significant differences ***$p < 0.001$, **$p < 0.01$, and *$p < 0.05$. Ordinary one-way ANOVA (MTT assay) and non-parametric Kruskal-Wallis test (DNA quantification)

These results are in line with those found in the literature, i.e., modified GG is not cytotoxic over different cell types [53–55].

Qualitative analysis of the morphology of chondrogenic primary cells in contact with Ty-GG hydrogel extracts was obtained by fluorescence microscopy (Fig. 7).

Chondrogenic primary cells were cultured with different conditions of extraction fluid of Ty-GG hydrogels. It was possible to verify that none of the conditions produced affected the typical morphology of the chondrogenic cells (marked by DAPI and phalloidin), suggesting healthy proliferation and survival.

Then, the rates of the pro-inflammatory tumor necrosis factor alfa (TNF-α), present in the medium after being in contact with Ty-GG hydrogels, were assessed. This cytokine is found in large quantities in patients with RA and has been studied with a therapeutic target. THP-1 cell line was differentiated with PMA and stimulated with LPS to assess the capacity of Ty-GG hydrogels encapsulated with betamethasone to decrease the levels of TNF-α present in the medium. Only C1 and C2 were analyzed regarding the neutralizing capacity since these were the best conditions in previous metabolic activity and cell proliferation. After the inflammation is manifested, 7 conditions were established to test, cells stimulated with LPS, without treatment, betamethasone alone, Ty-GG hydrogels (C1 and C2) without betamethasone encapsulated, and Ty-GG hydrogels (C1 and C2) encapsulated with betamethasone. Cells differentiated with PMA but without LPS stimulation were used as control.

Figure 8 shows the graphs of C1 (a) and C2 (b) separately, regarding the amount of TNF-α present in RPMI medium for 1 day, 3 days, and 7 days of culturing.

The results showed that cells stimulated with LPS but without treatment demonstrated high levels of free TNF-α in the RPMI medium, compared with the other conditions. Furthermore, it was possible to verify a higher neutralization of TNF-α in THP-1 cells treated with Ty-GG hydrogels encapsulated with betamethasone (C1 and C2) than with Ty-GG (C1 and C2) and betamethasone alone (C1 and C2). Significant differences were found between cells stimulated with LPS without treatment and cells that were treated Ty-GG hydrogels encapsulated with betamethasone (*$p < 0.05$). This significant difference was more evident in C1 than C2, at the first time point.

The higher ability to neutralize the TNF-α becomes more noticeable on the 7th day, which may be because hydrogels are degrading, so a higher amount of drug is released.

Ty-GG hydrogels loaded with betamethasone can bring more advantages in the treatment of the inflammatory environment than the drug alone. This approach may allow a prolonged action, due to the controlled rate of drug release over time, and treat inflammation more effectively in patients with RA. Furthermore, as mentioned earlier, it can reduce frequent administration of the drug to patients, decreasing the level of toxicity caused by recurrent administrations.

The data is in agreement with the previously reported literature [56–58] where it was shown a great potential of GG for distinct applications, such as mucoadhesive, transdermal and colon targeted controlled drug release systems.

Conclusion

This study developed tyramine-substituted gellan gum hydrogels via enzymatic and physical crosslinking, where betamethasone encapsulated can increase the specificity and safety in the treatment of patients with RA. The gellan gum was effectively modified with tyramine, presenting a substitution degree of about 30%. Tyramine-substituted gellan gum hydrogels showed rapid gelation time and demonstrated a good strength and resistance, ideal to be applied in the intra-

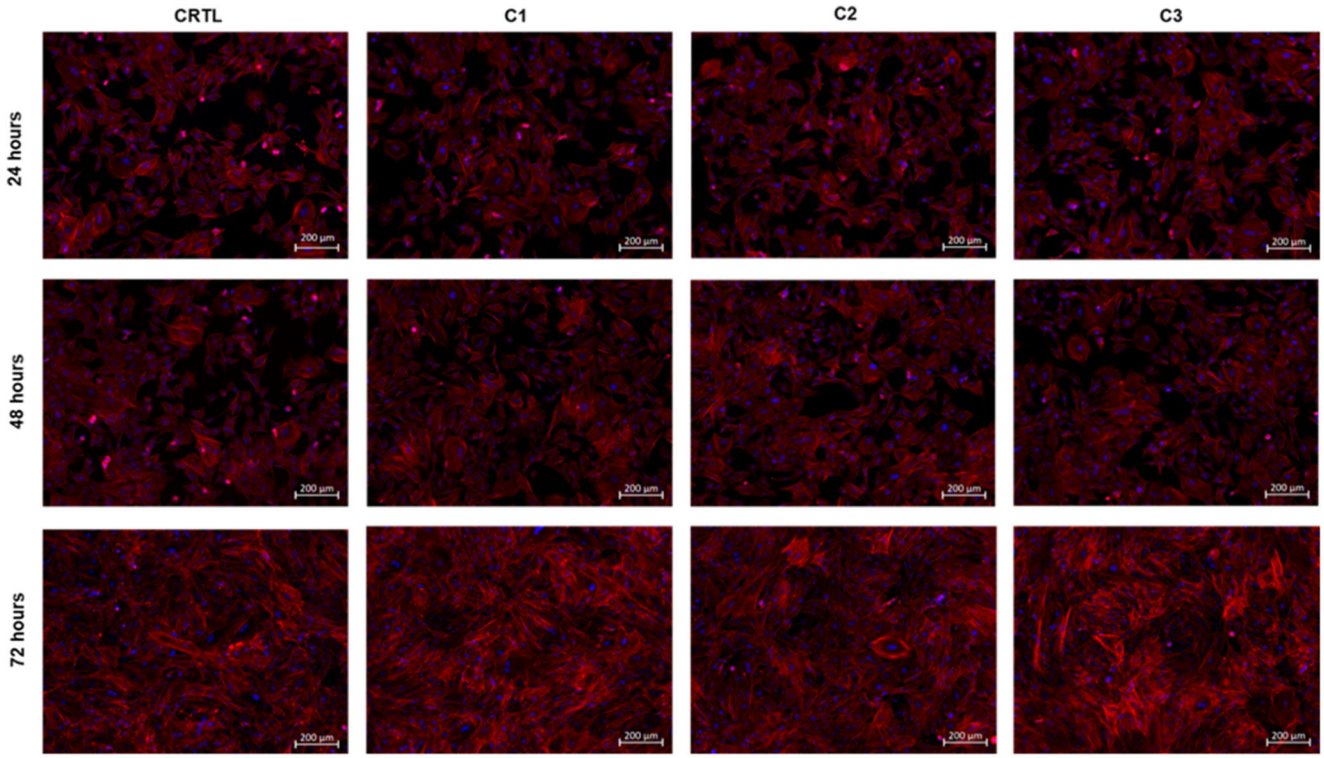

Fig. 7 Fluorescence microscopy images of chondrogenic primary cells cultured in the presence of CRTL (RMPI medium) and C1, C2, and C3 of Ty-GG hydrogels for 72 h. Scale bar: 200 μm

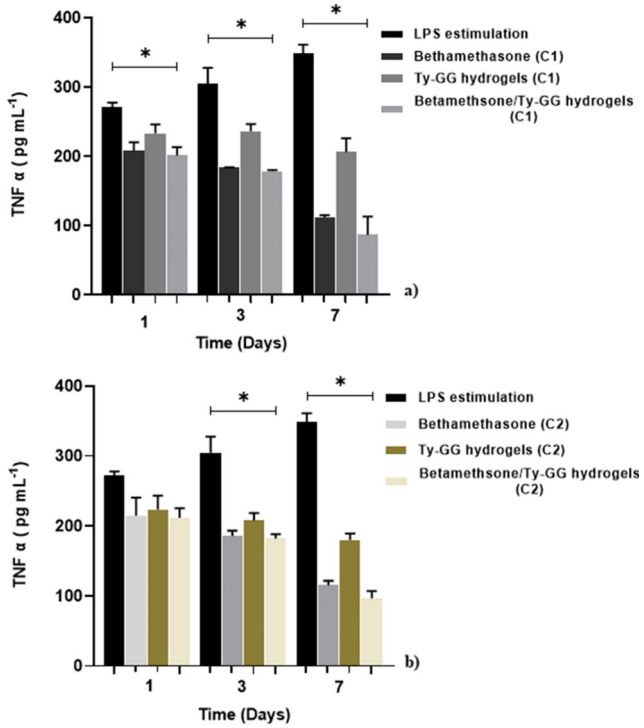

Fig. 8 Amount of TNF-α present in the medium, in contact with different conditions, cells stimulated with LPS, betamethasone (C1); Ty-GG hydrogels (C1) and Ty-GG hydrogels (C1) encapsulated with betamethasone (**a**). Cells stimulated with LPS, betamethasone (C2), Ty-GG hydrogels (C2) and Ty-GG hydrogels (C2) encapsulated with betamethasone (**b**). Significant differences $***p < 0.001$, $**p < 0.01$ and $*p < 0.05$, non-parametric Kruskal-Wallis test

articular cavity. The tyramine-substituted gellan gum hydrogels presented low water absorption capacity, a constant weight loss profile, and a controlled betamethasone release profile over time. Thus, it can be considered that the properties of gellan gum were improved after modification. Furthermore, the tyramine-substituted gellan gum hydrogels did not show to cause toxic effects on metabolic activity, morphology, and cell proliferation, and tyramine-substituted gellan gum hydrogels with betamethasone encapsulated demonstrated more effective therapeutic efficacy over time than betamethasone alone. Therefore, tyramine-substituted gellan gum hydrogel has excellent potential to be used as a drug delivery system for the treatment of rheumatoid arthritis.

Acknowledgments I. Oliveira thanks the financial support under the Norte2020 project ("NORTE-08-5369-FSE-000044"), REMIX project (G.A. 778078 — REMIX — H2020-MSCA-RISE-2017), and Gilson Lab, Chonbuk National University, Republic of Korea. The FCT distinction attributed to J. Miguel Oliveira under the Investigator FCT program (IF/01285/2015) is also greatly acknowledged. C. Gonçalves also wish to acknowledge FCT for supporting her research (No. SFRH/BPD/94277/2013).

Compliance with ethical standards

Conflict of interest The authors declare that they have no conflict of interest.

Ethical standards The experiments comply with the current laws of the country in which they were performed.

Animal studies The national and institutional guidelines and certification for the animal experimentation were followed as approved by the Direcção Geral de Alimentação e Veterinária (DGAV) and following the local ethical committee recommendations.

References

1. Wang M, Wei J, Li H, Ouyang X, Sun X, Tang Y, et al. Leptin upregulates peripheral CD4+ CXCR5+ ICOS+ T cells via increased IL-6 in rheumatoid arthritis patients. J Interf Cytokine Res. 2018;38(2):86–92.
2. Guo Q, Wang Y, Xu D, Nossent J, Pavlos NJ, Xu J. Rheumatoid arthritis: pathological mechanisms and modern pharmacologic therapies. Bone Res. 2018;6(1):1–14.
3. Pirmardvand Chegini S, Varshosaz J, Taymouri S. Recent approaches for targeted drug delivery in rheumatoid arthritis diagnosis and treatment. Artif Cells Nanomed Biotechnol. 2018;46(sup2):502–14.
4. Andersen NS, Cadahia JP, Previtali V, Bondebjerg J, Hansen CA, Hansen AE, et al. Methotrexate prodrugs sensitive to reactive oxygen species for the improved treatment of rheumatoid arthritis. Eur J Med Chem. 2018;156:738–46.
5. Gouveia VM, Lima SCA, Nunes C, Reis S. Non-biologic nanodelivery therapies for rheumatoid arthritis. J Biomed Nanotechnol. 2015;11(10):1701–21.
6. Yang M, Feng X, Ding J, Chang F, Chen X. Nanotherapeutics relieve rheumatoid arthritis. J Control Release. 2017;252:108–24.
7. Prosperi D, Colombo M, Zanoni I, Granucci F, editors. Drug nanocarriers to treat autoimmunity and chronic inflammatory diseases. Semin Immunol; 2017: Elsevier.
8. Feng X, Chen Y. Drug delivery targets and systems for targeted treatment of rheumatoid arthritis. J Drug Target. 2018;26(10):845–57.
9. Hoare TR, Kohane DS. Hydrogels in drug delivery: progress and challenges. Polymer. 2008;49(8):1993–2007.
10. Li J, Mooney DJ. Designing hydrogels for controlled drug delivery. Nat Rev Mater. 2016;1(12):1–17.
11. Xu Y, Li Y, Chen Q, Fu L, Tao L, Wei Y. Injectable and self-healing chitosan hydrogel based on imine bonds: design and therapeutic applications. Int J Mol Sci. 2018;19(8):2198.
12. Yang J-A, Yeom J, Hwang BW, Hoffman AS, Hahn SK. In situ-forming injectable hydrogels for regenerative medicine. Prog Polym Sci. 2014;39(12):1973–86.
13. Harding NE, Patel YN, Coleman RJ. Organization of genes required for gellan polysaccharide biosynthesis in Sphingomonas elodea ATCC 31461. J Ind Microbiol Biotechnol. 2004;31(2):70–82.
14. Shin H, Olsen BD, Khademhosseini A. Gellan gum microgel-reinforced cell-laden gelatin hydrogels. J Mater Chem B. 2014;2(17):2508–16.
15. Hu W, Wang Z, Xiao Y, Zhang S, Wang J. Advances in crosslinking strategies of biomedical hydrogels. Biomater Sci. 2019;7(3):843–55.
16. Li X, Sun Q, Li Q, Kawazoe N, Chen G. Functional hydrogels with tunable structures and properties for tissue engineering applications. Front Chem. 2018;6:499.
17. Parhi R. Cross-linked hydrogel for pharmaceutical applications: a review. Adv Pharm Bull. 2017;7(4):515–30.
18. Akhtar MF, Hanif M, Ranjha NM. Methods of synthesis of hydrogels… a review. Saudi Pharm J. 2016;24(5):554–9.
19. Khanmohammadi M, Dastjerdi MB, Ai A, Ahmadi A, Godarzi A, Rahimi A, et al. Horseradish peroxidase-catalyzed hydrogelation for biomedical applications. Biomater Sci. 2018;6(6):1286–98.
20. Lee F, Bae KH, Kurisawa M. Injectable hydrogel systems crosslinked by horseradish peroxidase. Biomed Mater. 2015;11(1):014101.
21. Ribeiro VP. Multifunctional silk fibroin-based constructs for tissue engineering and regenerative medicine applications. [Doctoral dissertation]. [Guimarães, PT]: Minho University; 2018.
22. Ribeiro VP, da Silva MA, Maia FR, Canadas RF, Costa JB, Oliveira AL, et al. Combinatory approach for developing silk fibroin scaffolds for cartilage regeneration. Acta Biomater. 2018;72:167–81.
23. Bae JW, Choi JH, Lee Y, Park KD. Horseradish peroxidase-catalysed in situ-forming hydrogels for tissue-engineering applications. J Tissue Eng Regen Med. 2015;9(11):1225–32.
24. Oryan A, Kamali A, Moshiri A, Baharvand H, Daemi H. Chemical crosslinking of biopolymeric scaffolds: current knowledge and future directions of crosslinked engineered bone scaffolds. Int J Biol Macromol. 2018;107:678–88.
25. Prodanovic O, Spasojevic D, Prokopijevic M, Radotic K, Markovic N, Blazic M, et al. Tyramine modified alginates via periodate oxidation for peroxidase induced hydrogel formation and immobilization. React Funct Polym. 2015;93:77–83.
26. Coutinho DF, Sant SV, Shin H, Oliveira JT, Gomes ME, Neves NM, et al. Modified gellan gum hydrogels with tunable physical and mechanical properties. Biomaterials. 2010;31(29):7494–502.
27. Reys LL, Silva SS, Soares da Costa D, Oliveira NM, Mano Jo F, Reis RL, et al. Fucoidan hydrogels photo-cross-linked with visible radiation as matrices for cell culture. ACS Biomater Sci Eng. 2016;2(7):1151–61.
28. Kim K, Park S, Yang J-A, Jeon J-H, Bhang S, Kim B-S, et al. Injectable hyaluronic acid–tyramine hydrogels for the treatment of rheumatoid arthritis. Acta Biomater. 2011;7(2):666–74.
29. Darr A, Calabro A. Synthesis and characterization of tyramine-based hyaluronan hydrogels. J Mater Sci Mater Med. 2009;20(1):33–44.
30. Loebel C, D'Este M, Alini M, Zenobi-Wong M, Eglin D. Precise tailoring of tyramine-based hyaluronan hydrogel properties using DMTMM conjugation. Carbohydr Polym. 2015;115:325–33.
31. Wennink JW, Niederer K, Bochyńska AI, Moreira Teixeira LS, Karperien M, Feijen J et al., editors. Injectable hydrogels by enzymatic co-crosslinking of dextran and hyaluronic acid tyramine conjugates. Macromol Symp; 2011: Wiley Online Library.
32. Prokopijevic M, Prodanovic O, Spasojevic D, Kovacevic G, Polovic N, Radotic K, et al. Tyramine-modified pectins via periodate oxidation for soybean hull peroxidase induced hydrogel formation and immobilization. Appl Microbiol Biotechnol. 2017;101(6):2281–90.
33. Jagur-Grodzinski J. Polymeric gels and hydrogels for biomedical and pharmaceutical applications. Polym Adv Technol. 2010;21(1):27–47.
34. Huang Y, Yu H, Xiao C. pH-sensitive cationic guar gum/poly (acrylic acid) polyelectrolyte hydrogels: swelling and in vitro drug release. Carbohydr Polym. 2007;69(4):774–83.
35. da Silva LP, Cerqueira MT, Sousa RA, Reis RL, Correlo VM, Marques AP. Engineering cell-adhesive gellan gum spongy-like hydrogels for regenerative medicine purposes. Acta Biomater. 2014;10(11):4787–97.
36. Flory PJ. Thermodynamics of high polymer solutions. J Chem Phys. 1941;9(8):660.
37. Jin R, Hiemstra C, Zhong Z, Feijen J. Enzyme-mediated fast in situ formation of hydrogels from dextran–tyramine conjugates. Biomaterials. 2007;28(18):2791–800.
38. Nguyen QV, Park JH, Lee DS. Injectable polymeric hydrogels for the delivery of therapeutic agents: a review. Eur Polym J. 2015;72:602–19.
39. Jin R, Lin C, Cao A. Enzyme-mediated fast injectable hydrogels based on chitosan-glycolic acid/tyrosine: preparation,

characterization, and chondrocyte culture. Polym Chem. 2013;5. https://doi.org/10.1039/C3PY00864A.
40. Buitrago-Vásquez M, Ossa-Orozco CP. Degradation, mater uptake, injectability and mechanical strength of injectable bone substitutes composed of silk fibroin and hydroxyapatite nanorods. Rev Fac the Ing. 2018;27(48):49–60.
41. Nam JG, Hyun K, Ahn KH, Lee SJ. Phase angle of the first normal stress difference in oscillatory shear flow. Korea-Aust Rheol J. 2010;22(4):247–57.
42. Ngan CL, Basri M, Lye FF, Masoumi HRF, Tripathy M, Karjiban RA, et al. Comparison of process parameter optimization using different designs in nanoemulsion-based formulation for transdermal delivery of fullerene. Int J Nanomedicine. 2014;9:4375.
43. Cai Z, Zhang H, Wei Y, Wu M, Fu A. Shear-thinning hyaluronan-based fluid hydrogels to modulate viscoelastic properties of osteoarthritis synovial fluids. Biomater Sci. 2019;7(8):3143–57.
44. Galesso D, Finelli I, Paradossi G, Renier D. Viscoelastic properties and elastic recovery of HYADD® 4 hydrogel compared to crosslinked HA-based commercial viscosupplements. Osteoarthr Cartil. 2012;20:S292.
45. Lawless BM, Sadeghi H, Temple DK, Dhaliwal H, Espino DM, Hukins DW. Viscoelasticity of articular cartilage: analysing the effect of induced stress and the restraint of bone in a dynamic environment. J Mech Behav Biomed Mater. 2017;75:293–301.
46. Risbud MV, Bhonde RR. Polyacrylamide-chitosan hydrogels: in vitro biocompatibility and sustained antibiotic release studies. Drug Deliv. 2000;7(2):69–75.
47. Li J, Mooney DJ. Designing hydrogels for controlled drug delivery. Nat Rev Mater. 2016;1(12):16071.
48. Zhang J, Ma PX. Cyclodextrin-based supramolecular systems for drug delivery: recent progress and future perspective. Adv Drug Deliv Rev. 2013;65(9):1215–33.
49. Dreyer SJ, Beckworth WJ. 2 - Commonly used medications in procedures. In: Lennard TA, Walkowski S, Singla AK, Vivian DG, editors. Pain Procedures in Clinical Practice. Third ed. Saint Louis: Hanley & Belfus; 2011. p. 5–12.
50. Jacobs JWG, Bijlsma JWJ. Chapter 60 - Glucocorticoid therapy. In: Firestein GS, Budd RC, Gabriel SE, IB MI, O'Dell JR, editors. Kelley and Firestein's Textbook of Rheumatology. Tenth ed: Elsevier; 2017. p. 932–57.e5.
51. Wernecke C, Braun HJ, Dragoo JL. The effect of intra-articular corticosteroids on articular cartilage: a systematic review. Orthop J Sports Med. 2015;3(5):2325967115581163. https://doi.org/10.1177/2325967115581163.
52. Østergaard M, Halberg P. Intra-articular corticosteroids in arthritic disease. BioDrugs. 1998;9(2):95–103. https://doi.org/10.2165/00063030-199809020-00002.
53. Silva-Correia J, Oliveira JM, Caridade S, Oliveira JT, Sousa R, Mano J, et al. Gellan gum-based hydrogels for intervertebral disc tissue-engineering applications. J Tissue Eng Regen Med. 2011;5(6):e97–e107.
54. Khang G, Lee S, Kim H, Silva-Correia J, Gomes ME, Viegas C, et al. Biological evaluation of intervertebral disc cells in different formulations of gellan gum-based hydrogels. J Tissue Eng Regen Med. 2015;9(3):265–75.
55. Silva-Correia J, Zavan B, Vindigni V, Oliveira MB, Mano J, Pereira H et al. Mechanical performance and biocompatibility study of methacrylated gellan gum hydrogels with potential for nucleus pulposus regeneration. J Tissue Eng Regen Med. 2012;6(2):18.
56. Kesavan K, Nath G, Pandit J. Preparation and in vitro antibacterial evaluation of gatifloxacin mucoadhesive gellan system. Daru. 2010;18(4):237.
57. Carmona-Moran C, Zavgorodnya O, Penman A, Kharlampieva E, Bridges S, Hergenrother R, et al. Development of gellan gum containing formulations for transdermal drug delivery: component evaluation and controlled drug release using temperature responsive nanogels. Int J Pharm. 2016;509:465–76. https://doi.org/10.1016/j.ijpharm.2016.05.062.
58. Norazemi N, Che Rose L, Rose, Mat Amin KA, Suhaimi H, Chan S-Y. Coated gellan gum hydrogel as a drug carrier for colon targeted drug delivery. J Sustain Sci Manag. 2017;2:36–41.